

A new method to detect long term trends of methane (CH₄) and nitrous oxide (N₂O) total columns measured within the NDACC ground-based high resolution solar FTIR network

J. Angelbratt¹, J. Mellqvist¹, T. Blumenstock⁵, T. Borsdorff⁴, S. Brohede¹, P. Duchatelet², F. Forster⁴, F. Hase⁵, E. Mahieu², D. Murtagh¹, A. K. Petersen^{3,*}, M. Schneider⁵, R. Sussmann⁴, and J. Urban¹

¹Chalmers University of Technology, Göteborg, Sweden

²Institute of Astrophysics and Geophysics, University of Liège, Liège, Belgium

³Institute of Environmental Physics, University of Bremen, Bremen, Germany

⁴Karlsruhe Institute of Technology (KIT), Institute for Meteorology and Climate Research (IMK-ASF), Garmisch-Partenkirchen, Germany

⁵Karlsruhe Institute of Technology (KIT), Institute for Meteorology and Climate Research (IMK-ASF), Karlsruhe, Germany

* present address: Max-Planck-Institute for Meteorology, Hamburg, Germany

Received: 21 December 2010 – Published in Atmos. Chem. Phys. Discuss.: 10 March 2011

Revised: 14 June 2011 – Accepted: 20 June 2011 – Published: 1 July 2011

Abstract. Total columns measured with the ground-based solar FTIR technique are highly variable in time due to atmospheric chemistry and dynamics in the atmosphere above the measurement station. In this paper, a multiple regression model with anomalies of air pressure, total columns of hydrogen fluoride (HF) and carbon monoxide (CO) and tropopause height are used to reduce the variability in the methane (CH₄) and nitrous oxide (N₂O) total columns to estimate reliable linear trends with as small uncertainties as possible. The method is developed at the Harestua station (60° N, 11° E, 600 m a.s.l.) and used on three other European FTIR stations, i.e. Jungfraujoch (47° N, 8° E, 3600 m a.s.l.), Zugspitze (47° N, 11° E, 3000 m a.s.l.), and Kiruna (68° N, 20° E, 400 m a.s.l.). Linear CH₄ trends between 0.13 ± 0.01–0.25 ± 0.02 % yr⁻¹ were estimated for all stations in the 1996–2009 period. A piecewise model with three separate linear trends, connected at change points, was used to estimate the short term fluctuations in the CH₄ total columns. This model shows a growth in 1996–1999 followed by a period of steady state until 2007. From 2007 until 2009 the atmospheric CH₄ amount increases between 0.57 ± 0.22–1.15 ± 0.17 % yr⁻¹. Linear N₂O trends between 0.19 ± 0.01–0.40 ± 0.02 % yr⁻¹ were estimated for all stations in the 1996–2007 period, here with the strongest trend at Harestua and Kiruna and the lowest at the Alp

stations. From the N₂O total columns crude tropospheric and stratospheric partial columns were derived, indicating that the observed difference in the N₂O trends between the FTIR sites is of stratospheric origin. This agrees well with the N₂O measurements by the SMR instrument onboard the Odin satellite showing the highest trends at Harestua, 0.98 ± 0.28 % yr⁻¹, and considerably smaller trends at lower latitudes, 0.27 ± 0.25 % yr⁻¹. The multiple regression model was compared with two other trend methods, the ordinary linear regression and a Bootstrap algorithm. The multiple regression model estimated CH₄ and N₂O trends that differed up to 31 % compared to the other two methods and had uncertainties that were up to 300 % lower. Since the multiple regression method were carefully validated this stresses the importance to account for variability in the total columns when estimating trend from solar FTIR data.

1 Introduction

Methane (CH₄) and nitrous oxide (N₂O) are among the largest contributors to the greenhouse effect (IPCC, 2007).

The CH₄ concentration in the atmosphere is to a large extent determined by the removal caused by the hydroxyl radical (OH) in the troposphere and the strength of the surface emissions (Dlugokencky et al., 1994). The emission sources are due to microbial activity primarily under anaerobic conditions in wetlands, rice paddies and landfills. Other



Correspondence to: J. Mellqvist
(johan.mellqvist@chalmers.se)

important CH₄ emission sources are ruminants, natural gas leakage and fossil fuel and biomass burning. The amount of CH₄ in the atmosphere has increased during the later part of the twentieth century. Between 1978–1987 in situ measurements has shown that the growth rate was important, (i.e. 1.1 % yr⁻¹), but during the late 1980 the growth rate was slowing down to 0.3–0.6 % yr⁻¹ and even lower growth rates were reported during the 1990s (Simpson et al., 2006). In the early 2000s the CH₄ growth rate was nearly zero. During 2007 and 2008 however, CH₄ was on the rise again and global growth rates of 0.47 ± 0.04 % yr⁻¹ and 0.25 ± 0.04 % yr⁻¹ were reported each respective year (Dlugokencky et al., 2009).

In contrast to CH₄, the dominant N₂O source, both natural and anthropogenic, is microbial activity in soils. The source is strongly linked with the use of synthetic nitrogen fertilizers, which have increased during the later part of the twentieth century (Davidson, 2009). Other important N₂O sources include: biomass burning, sewers, livestock and emission from transport and industries. The main sink for N₂O is photodissociation in the stratosphere by ultraviolet light and reaction with excited oxygen atoms (Bates and Hays, 1967). Compared to the CH₄ trend, the N₂O accumulation in the atmosphere has been continuous. During the last three decades, the atmospheric N₂O burden has shown an almost (constant) linear increase with a reported annual change of 0.26 % yr⁻¹ (IPCC, 2007).

This paper was carried out within the EU project HYMN (Hydrogen, Methane and Nitrous Oxide, <http://www.knmi.nl/samenw/hymn/>) and one of the goals was to improve and homogenize the CH₄ and N₂O retrievals from high-resolution solar FTIR (Fourier Transform Infra Red) measurements and to obtain, for both gases, total columns and vertical profiles as accurately as possible. Many of the participating ground-based FTIR stations have time series that cover 15 years of data or more and it is therefore possible and interesting to study long term trends. Trends from greenhouse gases from FTIR measurements have earlier also been performed within the EU project UFTIR (<http://www.nilu.no/uftir/>) (Vigouroux et al., 2008).

One advantage when using FTIR total columns for the estimation of long term trends is their insensitivity to local variations of the atmosphere. In addition, since the global circulation is zonal in the free troposphere and stratosphere, the air stays at approximately the same latitude and the measurement station will therefore represent the atmosphere at that latitude. Hence, only a few stations at different latitudes are needed to represent the whole atmosphere. One disadvantage with FTIR is the fact that the time series often are unevenly sampled since the solar absorption infrared measurements require clear sky conditions. Furthermore there are, for some stations, periods of missing data due to instrument failure and for the most northern stations because of the polar winter.

One of the common methods for estimating trends of atmospheric parameters is to use monthly average values (see

for example Jones et al., 2009). The use of this method reduces the variability in the time series and removes the eventual periods of missing data. For an evenly sampled time series it is also possible to take the autocorrelation (also called serial correlation) into account (Tiao et al., 1990; Weatherhead et al., 1998). The FTIR data are autocorrelated on different timescales e.g., caused by meteorological patterns, seasonal cycles and other kinds of long-term variability. This correlation can best be described as a memory in the time series where a value at a certain time contains information of earlier values. Since our present FTIR time series include both unevenly sampling and in some instance significant gaps it is difficult to create representative monthly averages. It is for some stations even impossible without interpolation. We use instead a multiple regression model, including a linear trend, a seasonal component and anomalies from various atmospheric parameters to account for the time series variability and autocorrelation to estimate reliable trends. The method also gives a possibility to quantify the atmospheric parameters that affect the measured time series through their contributions to the fitted regression model.

2 FTIR measurements and data retrieval

In this paper we use total column time series of CH₄, N₂O, carbon monoxide (CO), hydrogen fluoride (HF) and ethane (C₂H₆) measured with FTIR spectrometers at four European stations, i.e. Jungfraujoch, Zugspitze, Harestua and Kiruna, within the NDACC network (Network for the Detection of Atmospheric Composition Change, <http://www.ndsc.ncep.noaa.gov/>). FTIR measurements have been performed since the mid 1990s, both in the Northern and Southern hemispheres. Information about the stations, instrumentations and retrievals are presented in Table 1. The CH₄ and N₂O trend analysis cover the 1996–2009 and 1996–2007 time periods, for respectively species.

All the FTIR spectrometers involved in this study operate in the mid infrared spectral region from 700 cm⁻¹ to 5000 cm⁻¹ (2 to 14 μm) and measure the molecular absorption of solar light in the atmosphere for a wide range of species. Derived atmospheric abundance is expressed in terms of total column, defined as the sum of molecules from the top of the atmosphere down to the measurement station, per unit area (often expressed as molecules per square centimetre). To be able to spectrally resolve the atmospheric absorption lines for a given species, high resolution spectrometers are needed. For the stations in this paper a typical spectral resolution of 0.0035–0.005 cm⁻¹ is used.

During the retrieval process a synthetic spectrum, based on a priori information of pressure, temperature, trace gas profiles and instrumental characteristics, is calculated, by utilizing a forward model, dividing the atmosphere into 41–66 layers and calculating the light propagation through these. The calculated spectrum is then fitted to the FTIR measurements

Table 1. FTIR stations included in the trend study.

	Jungfrauoch	Zugspitze	Harestua	Kiruna
Latitude (° N)	47	47	60	68
Longitude (° E)	8	11	11	20
Altitude (m a.s.l)	3600	3000	600	400
Instrument type	Bruker 120HR	Bruker 125HR ^a	Bruker 125M ^b	Bruker 125HR ^c
Retrieval code	SFIT2	SFIT2	SFIT2	PROFFIT
No. of measurement days, CH ₄	1135	818	599	642
No. of measurement days, N ₂ O	1160	739	592	765

^a before 2006 Zugspitze operated a Bruker 120HR, ^b before 2008 Harestua operated a Bruker 120M and ^c before 2007 Kiruna operated a Bruker 120HR.

by varying the mixing ratio profile of the target species together with interfering species such as H₂O and CO₂. In this manner vertical profile of the target species can be obtained. These are generally calculated into total columns using the available pressure and temperature information but for some species the data can also be divided into partial columns for instance dividing the total column into a tropospheric and stratospheric part. The height information available from the spectra is usually defined as the degrees of freedom (DOFs) which is obtained from averaging kernel calculations according to the principles described by Rodgers (2000).

The retrievals in this paper are performed by the two algorithms SFIT2 (Rinsland et al., 1998) and PROFFIT (Hase et al., 2004). The two codes have been shown to be in excellent agreement with a deviation of only 1 % or less (Hase et al., 2004). To quantify the instrument performance regarding line broadening and phase shift gas-cell measurements are done regularly on all instruments. These measurements are evaluated with the LINEFIT program (Hase et al., 1999).

The CH₄ and N₂O retrievals are done with a common strategy developed within the EU project HYMN, where the micro-windows, spectroscopic line lists, retrieval parameters, sources of ancillary data like pressure-temperature profiles, and water vapour data for deriving dry air columns are identical for all involved stations and used to minimize the biases between the stations.

In an earlier FTIR trend study by Gardiner et al. (2008), the retrievals were carried out by the optimal estimation algorithm (Rodgers, 2000). In this retrieval algorithm a cost function is minimized which corresponds to a weighted combination of a multiple least square solution and the a priori information. In the case of CH₄ and N₂O severe oscillations in the profiles are obtained and therefore instead a retrieval algorithm based on Tikhonov regularization (Twomey, 1996) has been applied to minimize this problem. In the latter retrieval algorithm, a cost function is minimized which corresponds to a weighted combination of a multiple least square solution and a cost term that corresponds to the first derivative of the vertical profile. The latter term minimises oscillations of the retrieved profile versus height but

Table 2. Microwindows with interfering species used to retrieve the CH₄ and N₂O total columns.

Species	Microwindows (cm ⁻¹)	Interfering species
CH ₄	2613.70–2615.40	HDO, CO ₂
	2650.60–2651.30	HDO, CO ₂
	2835.50–2835.80	
	2903.60–2904.03	NO ₂
	2921.00–2921.60	H ₂ O, HDO, NO ₂
N ₂ O	2481.28–2482.62	CO ₂ , CH ₄
	2526.40–2528.20	CO ₂ , CH ₄ , HDO
	2537.84–2538.82	CH ₄
	2540.00–2540.75	CH ₄

reduces the profile information to 2–3 independent partial columns (DOFs). For more information regarding FTIR retrieval with Tikhonov see Sussmann and Borsdorf (2007) and Sussmann et al. (2005).

In Table 2 information regarding the HYMN micro windows and interfering species are presented. For both CH₄ and N₂O Hitran 2004 linelist parameters are used.

The CO, C₂H₆ and HF total columns, used as atmospheric parameters in the multiple regression model, are retrieved with standard procedures that have earlier been developed within the NDACC community (Mellqvist et al., 2002) (De-Mazière et al., 2005). The retrieval procedure varies slightly from site to site but uses consistent micro window regions for CO (2057–2159 cm⁻¹), C₂H₆ (2976–2977 cm⁻¹) and HF (4038–4039 cm⁻¹).

3 The Odin satellite

The Sub-Millimeter Radiometer (SMR) onboard the Odin satellite, launched in February 2001, observes thermal emission of a N₂O line at 502.3 GHz at the Earth limb. Measurements of the global N₂O field are obtained during about 15 (near polar, sun-synchronous) orbits per observation day

and were performed time-shared with other operation modes on every third day until April 2007 and on every second day since then, providing a quasi-continuous N₂O data set from 2001 to 2010. N₂O in the stratosphere is retrieved between roughly 12–14 km and 60 km with a vertical resolution of about 1.5 km and a single-scan precision of 10–15 % (below 30 km). For the here relevant level-2 data version 2.1 See e.g. Murtagh et al. (2002); Urban et al. (2005b,a); Urban (2006); and Strong et al. (2008) for a description of the Odin mission and information of the N₂O measurements, error analysis and validation studies.

4 Trend method

4.1 Linear regression

Regression analysis is a technique to study the connection between a dependent variable and one or several independent variables. In this paper we mean the dependency between the independent variable, time, and the dependent variable, the measured total column time series. The simplest way to detect a trend is by fitting a straight line with the least squares method to the data, the slope of the line then represents the trend. The estimated trend itself is of limited use without an estimate of its error which could be represented with a confidence interval. When calculating a trend and its confidence interval three assumptions are usually made: (1) the residuals (measured-model) are assumed to be free from autocorrelation, (2) the distribution of the residuals is assumed to be approximately normally distributed and (3) the residuals are assumed to have equal variance. Large deviations from these assumptions will result in errors in the estimated trends and its confidence intervals (Weatherhead et al., 1998; Tiao et al., 1990). Methods have been developed to account for autocorrelation when estimating trends but they all need data which have equidistant time steps between the measurements. However, due to local weather conditions and available sunlight hour's time series derived from FTIR observations are not sampled evenly and typically contain gaps. It is hence not possible to make representative weekly or monthly averages and thereby get time series with constant time spacing. To reduce the time series variability and estimate reliable trends a multiple regression model is used in this paper.

4.2 Atmospheric parameters

Several atmospheric parameters that are assumed to affect the measured total column of CH₄ and N₂O are discussed in this section. Data from the Harestua station have been used to test the effect of various atmospheric parameters on the measured total columns of CH₄ and N₂O. The parameters that have shown to have a significant effect on the measured total columns of CH₄ and N₂O at the Harestua station have then been applied to the FTIR data from the other participating stations.

Changes in the *air pressure* due to meteorological fluctuations will change the amount of molecules above the measurement station. A high pressure is expected to result in a high total column and vice versa. CH₄ and N₂O have their highest partial columns close to ground level, where they are intensively produced, and are therefore expected to be very sensitive to fluctuations in the air pressure. The *tropopause height* is expected to affect the stratospheric column of CH₄ and N₂O but also to stretch and compress the tropospheric column. A low tropopause height is thought to make the tropospheric contribution to the total column smaller and a high larger. The tropopause height data used here are from the ECMWF (European Centre for Medium Range Weather Forecasts, <http://www.ecmwf.int/>) model that defines the tropopause altitude as the lowest level where the lapse rate is 2 °C km⁻¹ or less and no height within 2 km above this point exceeds this value. To account for the presence of the polar vortex a range of *PV (polar vorticity)* values, at different altitudes (10–25 km), is obtained from the ECMWF model. A high PV value is expected to correspond to the presence of vortex air above the measurements site and hence a low stratospheric column of CH₄ and N₂O.

The total column of the stratospheric species HF has been used in several other studies, among them Toon et al. (1997) and Mellqvist et al. (2002), as a proxy for stratospheric transport. This transport involves the downward motion of airmasses when the station is inside the polar vortex, the changes in tropopause height and the vertical and horizontal motion of air masses in the stratosphere. Hence, a large *total column of HF* is expected to result in a large stratospheric and a small tropospheric column of CH₄ and N₂O.

CH₄, N₂O, CO and C₂H₆ are all produced in fossil fuel and biomass burning. The *total columns of CO and C₂H₆* are therefore used as a proxy for large scale biomass burning events as the ones present in Canada and Russia during the summers of 1998, 1999, 2002 and 2003 (Yurganov et al., 2004,2005). The *total columns of C₂H₆* will in addition be used as a proxy for natural gas leakage. This has, as to our knowledge, not been tested on CH₄ and N₂O FTIR total columns before.

Other physical parameters that have been investigated are: the number of sunspots, the North Atlantic Oscillations (NAO) and the Quasi Biennial Oscillations (QBO).

4.3 Trend model

To estimate trends in the CH₄ and N₂O total column time series a multiple regression model is used. In the model we try to explain as much as possible of the structures in the measured total column of CH₄ and N₂O with atmospheric parameters, a background trend and a seasonal component. The background trend is represented by one or several continuous linear trends according to the piecewise regression concept described by Neter et al. (1990). The seasonal component consists of a sine function with a phase which has a period

of 12 months. The 12 month seasonal cycle is strongest at the high altitude stations due to the well mixed air i.e. the low influence of local sources. A more advanced representation of the seasonal cycle, a third order Fourier series, has also been tested in the model but did not improve the model compared to the basic one. To explain the time series variability, i.e. short term deviations from the background trend and seasonal fluctuations, anomalies derived from some of the atmospheric parameters described in Sect. 4.2 are used. These anomalies correspond to the detrended and deseasonalized time series of the atmospheric parameters.

To find the anomalies that affect the CH₄ and N₂O total columns all derived anomalies are inserted into the multiple regression model, presented in Eq. (1), and tested with the stepwise regression method. This means that the combination of anomalies that gives the best adjusted R^2 value and are statistically significant are used in the final trend model and all the others being excluded. We define statistically significant as a parameter for which the confidence interval excludes zero on a 2- σ level.

To estimate trends the anomalies found with the stepwise approach, the background trend and the seasonal component are inserted in the model in Eq. (1) and solved with the least squares method.

$$y = \beta_0 + \beta_1 \sin(2\pi t) + \beta_2 \cos(2\pi t) + \sum_{i=3}^I \beta_i a(t)_{i-2} + \beta_{I+1}t + \beta_{I+2}(t - \text{cp1})A + \beta_{I+3}(t - \text{cp2})B + \varepsilon$$

$$\text{where } \begin{cases} t > \text{cp1}, A = 1 \\ t \leq \text{cp1}, A = 0 \\ t > \text{cp2}, B = 1 \\ t \leq \text{cp2}, B = 0 \end{cases} \quad (1)$$

Where t is the time in fraction of years and cp1 and cp2 are change points when the trend is expected to change direction or magnitude. For CH₄, possible change points in 1999 and 2007 have been reported by Dlugokencky et al. (2003, 2009) who have made global in situ measurements. In a first trend estimation no change points will be used for CH₄ and N₂O while in a second estimation the change points of Dlugokencky et al. (2003, 2009) will be used for CH₄. When no change points are used only the first trend term in Eq. (1) will be present in the model. In Eq. (1) y is the dependent variable (CH₄ or N₂O) and β corresponds to the regression coefficients. The $a(t)_i$ terms represent the anomalies from the atmospheric parameters (i to I) and ε is the residual or unexplained part of the model. The term is assumed to be normal distributed with a constant variance around zero and free from auto correlation. In the regression model the anomalies, $a(t)_i$, t and y must all be of the same length. This means that for a certain day in the CH₄ or N₂O time series there must exist corresponding data for all of the calculated anomalies.

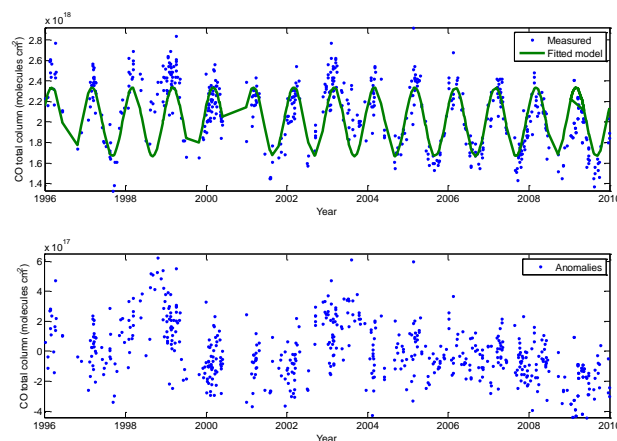


Fig. 1. Measured total column of CO at Harestua with fitted model (upper panel) and calculated anomalies (lower panel). To obtain the anomalies the fitted model is subtracted from the measured time series.

To estimate confidence intervals for the trends a method for hypothesis testing described by Montgomery et al. (2008) is used.

4.4 Deriving anomalies

To obtain anomalies from the atmospheric parameters presented in Sect. 4.2, a model consisting of a seasonal function and a polynomial with varying order is fitted to each of the atmospheric parameters, Eq. (2). The fitted model is then subtracted from the original atmospheric time series. To find the optimal polynomial fit for each atmospheric parameter the adjusted R^2 value is used (Montgomery et al., 2008). The value reflects the correlation between the model and the measurements and adjusts this correlation to the number of terms used in the regression model. If no adjustment is used the correlation always increase when increasing the number of terms in the regression model, this favours over fitting. An adjusted R^2 value close to one indicates a small residual and a good model fit while zero indicates the opposite.

$$y = \beta_0 + \beta_1 \sin(2\pi t) + \beta_2 \cos(2\pi t) + \beta_3 t + \beta_4 t^2 + \beta_5 t^3 \quad (2)$$

In Eq. (2) y is the dependent variable i.e. the atmospheric parameters (air pressure, tropopause height and so on) and β are the estimated regression coefficients. The optimal polynomial for each atmospheric process is found by step wise increasing the polynomial order, fit the models with the linear regression method and calculated the adjusted R^2 value. When the adjusted R^2 value no longer increases with more than 1 % the best fit is said to be found and the corresponding polynomial order is used to derive the anomaly. In Fig. 1 an example of the derived anomalies from the Harestua total column time series of CO is presented.

5 Results

5.1 Anomalies in the final regression model

The anomalies shown to affect the measured total columns of CH₄ are: the air pressure, the total column of CO and HF and the anomalies that affect the N₂O total columns are: the air pressure the total column of HF and the tropopause height. The air pressure, CO and tropopause height anomalies are derived using Eq. (2) along with a linear trend. For HF a second order polynomial is used in Eq. (2) for Harestua, Jungfraujoch and Zugspitze while a linear trend is used for the fit of the Kiruna dataset.

The stepwise regression model that was applied on the Harestua data showed a final model where C₂H₆ were included instead of CO, this due to a slightly higher adjusted R^2 value. At the time of performing the stepwise test not all stations were retrieving C₂H₆. Instead CO has to be used in the final model. Since C₂H₆ and CO shows a strong correlation this practical simplification was assumed to work properly. The linear correlations between all the tested anomalies are presented in Table 3. Except the CO-C₂H₆ correlation a slightly weaker correlation can be seen for the air pressure and the tropopause height. The other anomalies have much weaker or no linear correlations.

The final regression coefficients of the stepwise regression model for Harestua are presented in Table 4. In the table it can be seen that the air pressure and the total column of HF and CO is significant for both CH₄ and N₂O. PV375 is also significant for CH₄ and the tropopause height is significant for N₂O. Although their significance not all parameters are included in the final model due to the fact that the adjusted R^2 value not is improved.

The reduction of the variability in the CH₄ and N₂O time series due to the addition of anomalies are presented in Fig. 2a and b, respectively. The reduction is calculated by comparing the standard deviation of the residuals when only offset and linear trend/trends is fitted to the data with the standard deviations derived when each of the anomalies and the seasonal function is added to the trend model. The seasonal function accounts for a few to roughly 18 % of the variability of the two CH₄ cases. The value is slightly higher for N₂O which show up to 22 %. For both species the seasonal function has the greatest impact at Jungfraujoch and smallest at Harestua. In the two CH₄ cases the air pressure anomaly accounts for 30–40 % of the variability. The corresponding value for N₂O is roughly 30 %. The HF anomaly reduces the variability more for N₂O, ~11–18 %, than for CH₄, ~2–10 %. The anomalies from CO and tropopause height corresponds both to a variability reduction of a couple of percent each. There is still place for improvements in the trend model since 30–55 % of the variability is unexplained, depending on station and species. This has partly to do with the measurement noise from the instrument but most likely also with atmospheric processes not captured in this paper.

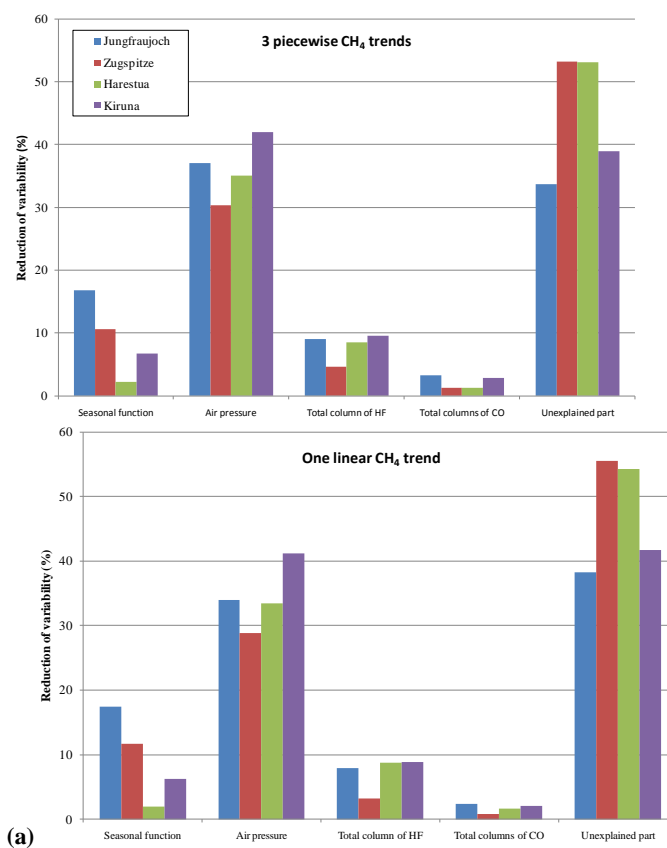


Fig. 2a. Reduction of the variability in the CH₄ time series from the anomalies and seasonal function in the regression model, presented as percent of total variability. The upper panel is when three piecewise trends are used and the lower is when a single linear trend is used.

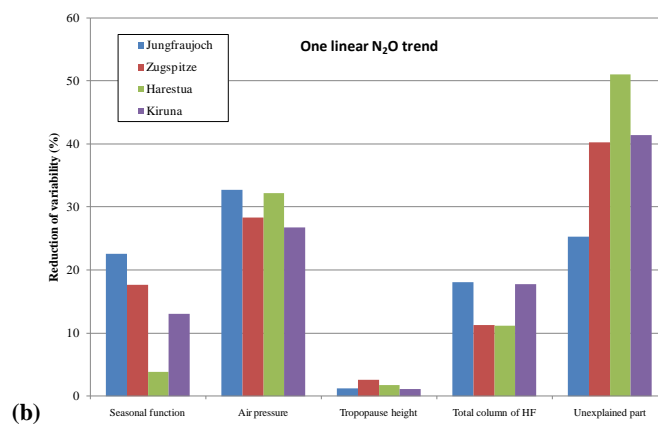
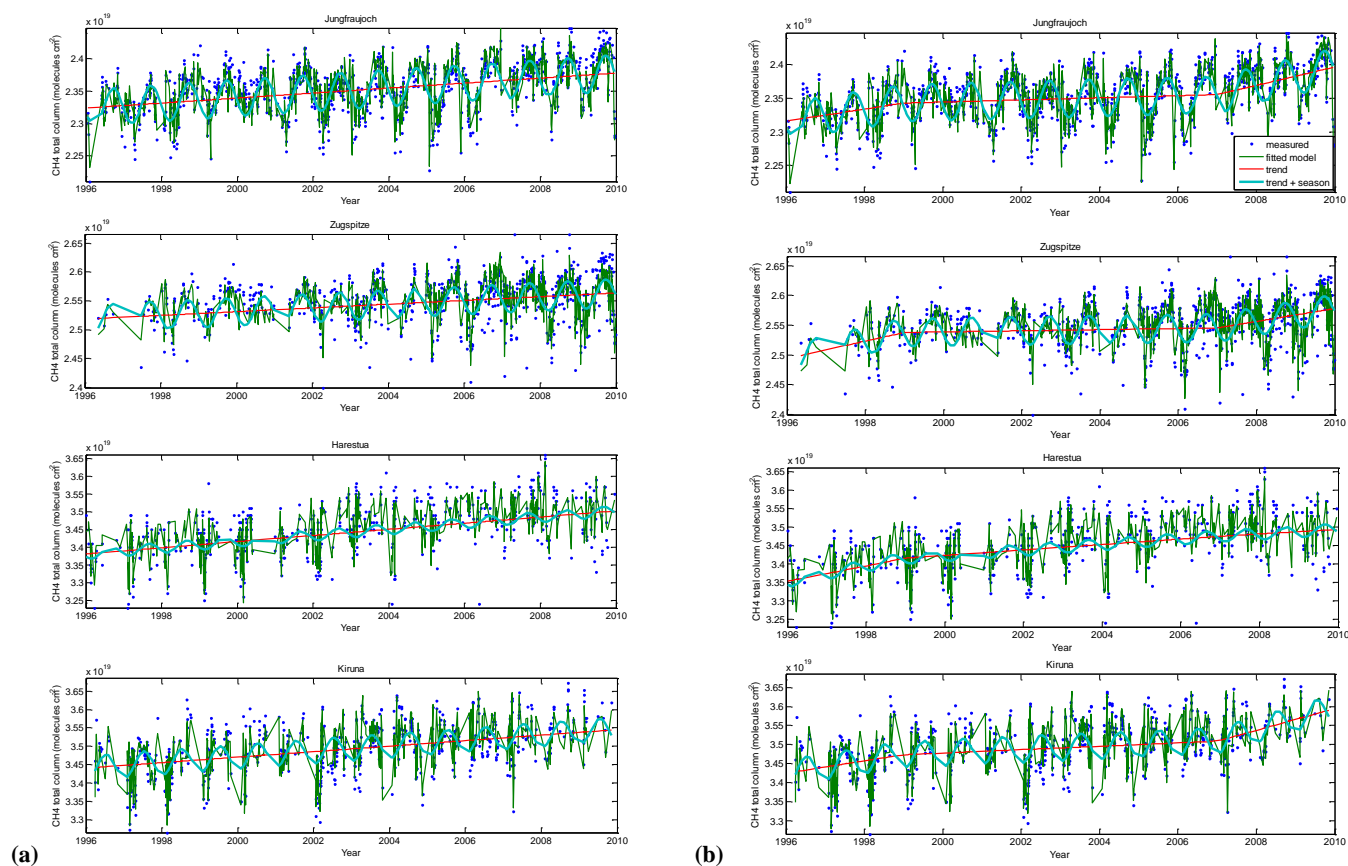


Fig. 2b. Reduction of the variability in the N₂O time series from the anomalies and seasonal function in the regression model, presented as percent of total variability.

It can be seen that the reduction of variability by each anomaly are fairly similar for all stations and species, this strengthens the choice of anomalies that are used in the trend

Table 3. Linear correlation calculated from the anomalies at the Harestua site. Correlations stronger or equal to 0.60 is marked in bold.

	CO	C ₂ H ₆	HF	Trop. h.	Air pres.	PV475	PV400	PV350	Sunsp.	NAO	QBO
CO	1.00	0.72	0.16	0.22	0.29	0.19	-0.04	-0.01	0.00	0.05	0.01
C ₂ H ₆	0.72	1.00	0.26	-0.11	0.00	0.24	-0.02	0.00	0.00	0.05	0.08
HF	0.16	0.26	1.00	-0.16	-0.21	0.51	-0.05	0.03	0.14	-0.07	-0.02
Trop. h.	0.22	-0.11	-0.16	1.00	0.60	0.13	0.02	-0.02	-0.08	0.03	-0.05
Air pres.	0.29	0.00	-0.21	0.60	1.00	0.03	-0.02	-0.04	-0.09	0.02	-0.07
PV475	0.19	0.24	0.51	0.13	0.03	1.00	0.04	0.02	-0.07	-0.08	-0.01
PV400	-0.04	-0.02	-0.05	0.02	-0.02	0.04	1.00	0.05	-0.04	0.00	0.05
PV350	-0.01	0.00	0.03	-0.02	-0.04	0.02	0.05	1.00	-0.05	-0.03	0.03
Sunsp.	0.00	0.00	0.14	-0.08	-0.09	-0.07	-0.04	-0.05	1.00	-0.09	0.04
NAO	0.05	0.05	-0.07	0.03	0.02	-0.08	0.00	-0.03	-0.09	1.00	0.01
QBO	0.01	0.08	-0.02	-0.05	-0.07	-0.01	0.05	0.03	0.04	0.01	1.00

**Fig. 3.** CH₄ total column time series for all participating FTIR stations with fitted model, linear trend and seasonal cycle. The model is displayed in green and the measurements in blue, the seasonal cycle is displayed in thick cyan and the linear trend in red.

model. Although the small variability reduction by CO and tropopause height that is showed in this paper these anomalies can have larger effects on the estimated trends if the start and/or end period is chosen when there is strong forest fires or atmospheric dynamics.

5.2 CH₄ trends

The estimated linear trends from the multiple regression model are presented in Table 5 and the fitted models to the CH₄ time series are presented in Fig. 3a for the linear trend and Fig. 3b for the piecewise linear trends. For all

Table 4. Regression coefficients with associated 2- σ confidence intervals of the stepwise regression model used on the CH₄ and N₂O total columns of the Harestua data. Statistical significant anomalies are marked in bold.

Anomaly	CH ₄	N ₂ O
CO	$9.8 \times 10^{15} \pm 4.0 \times 10^{15}$	$1.9 \times 10^{15} \pm 8.6 \times 10^{14}$
HF	$-1.4 \times 10^{16} \pm 1.8 \times 10^{15}$	$-3.4 \times 10^{15} \pm 4.0 \times 10^{14}$
Tropopause height	$2.1 \times 10^{15} \pm 3.2 \times 10^{15}$	$7.7 \times 10^{14} \pm 7.0 \times 10^{14}$
Air pressure	$3.3 \times 10^{17} \pm 2.8 \times 10^{16}$	$6.9 \times 10^{16} \pm 6.0 \times 10^{15}$
PV475	$2.6 \times 10^{14} \pm 1.4 \times 10^{15}$	$-2.2 \times 10^{13} \pm 2.9 \times 10^{14}$
PV400	$5.7 \times 10^{14} \pm 1.4 \times 10^{15}$	$-3.4 \times 10^{13} \pm 3.1 \times 10^{14}$
PV350	$2.0 \times 10^{15} \pm 1.4 \times 10^{15}$	$1.6 \times 10^{14} \pm 3.5 \times 10^{14}$
No. of sunspots	$-4.9 \times 10^{14} \pm 4.9 \times 10^{14}$	$9.4 \times 10^{13} \pm 7.9 \times 10^{13}$
NAO	$-3.6 \times 10^{12} \pm 2.3 \times 10^{13}$	$-1.7 \times 10^{11} \pm 5.8 \times 10^{11}$
QBO	$-2.2 \times 10^{12} \pm 2.6 \times 10^{13}$	$3.0 \times 10^{11} \pm 2.0 \times 10^{12}$

Table 5. Estimated linear trends from the multiple regression model. The trends are given as total column and as percent relative the average value of year 2000. The confidence limits for each trend are based on a 2- σ significance level.

Time period		Jungfraujoch (47° N, 8° E)	Zugspitze (47° N, 11° E)	Harestua (60° N, 11° E)	Kiruna (68° N, 20° E)	
CH ₄	1996–2009	$\text{mol cm}^{-2} 10^{16}$ $\% \text{ yr}^{-1}$	3.85 ± 0.13 0.16 ± 0.01	3.24 ± 0.29 0.13 ± 0.01	8.63 ± 0.52 0.25 ± 0.02	7.5 ± 0.38 0.21 ± 0.01
	1996–1999	$\text{mol cm}^{-2} 10^{16}$ $\% \text{ yr}^{-1}$	9.00 ± 0.92 0.38 ± 0.04	14.60 ± 0.95 0.57 ± 0.04	20.80 ± 3.53 0.61 ± 0.10	16.10 ± 2.65 0.46 ± 0.08
	1999–2007	$\text{mol cm}^{-2} 10^{16}$ $\% \text{ yr}^{-1}$	1.57 ± 1.97 0.07 ± 0.08	0.95 ± 1.96 0.04 ± 0.08	7.39 ± 7.54 0.22 ± 0.22	4.45 ± 5.68 0.13 ± 0.16
	2007–2009	$\text{mol cm}^{-2} 10^{16}$ $\% \text{ yr}^{-1}$	21.10 ± 1.79 0.90 ± 0.08	24.50 ± 1.34 0.96 ± 0.05	19.70 ± 7.54 0.57 ± 0.22	40.30 ± 5.92 1.15 ± 0.17
N ₂ O	1996–2007	$\text{mol cm}^{-2} 10^{15}$ $\% \text{ yr}^{-1}$	8.6 ± 0.26 0.21 ± 0.01	8.5 ± 0.56 0.19 ± 0.01	23.6 ± 1.25 0.40 ± 0.02	17.2 ± 1.40 0.29 ± 0.02

participating stations significant trends at the 2- σ level are found for the period of 1996–2009. The trends vary with latitude and weaker trends are observed at Jungfraujoch and Zugspitze ($0.16 \pm 0.01 \%$ yr⁻¹ and $0.13 \pm 0.01 \%$ yr⁻¹) and stronger trends at Harestua and Kiruna ($0.25 \pm 0.02 \%$ yr⁻¹ and $0.21 \pm 0.01 \%$ yr⁻¹). The trends at the Alpine stations are as expected in close agreement to each other due to their close geographical location. Earlier Gardiner et al. (2008) have estimated linear trends for FTIR data and these trends are close to the estimated ones in this paper, i.e. $0.40 \pm 0.06 \%$ yr⁻¹ for Harestua and $0.17 \pm 0.03 \%$ yr⁻¹ for Jungfraujoch. The data in the earlier paper corresponds to the years 1995–2004 and they were retrieved with standard optimal estimation as explained earlier and the trend were derived with the Bootstrap method, see discussion below.

Dlugokencky 2009 reports an increased CH₄ growth in 2007 and 2008 based on global averages from in situ flask

samples. The same author has also reported a near zero trend between 1999 and 2007 and a positive trend before that. To investigate if these features also are present in the FTIR data we have applied piecewise regression (Neter et al., 1990) with three independent linear trends, choosing 1999 and 2007 as changing points in the trend model, Table 5. For all stations significant positive CH₄ growth rates are found for the 1996–1999 time period. The estimated values are between 0.38% yr⁻¹ and 0.61% yr⁻¹. This could be compared with the globally averaged surface trend value of 0.45% yr⁻¹ based on the time period of 1984–1999 reported by Dlugokencky et al. (2003). For each station involved, no significant trends have been deduced for CH₄ for the 1999–2007 time period, this is in agreement with global surface CH₄ data for the time period of 2000–2006 (Dlugokencky et al., 2009). From 2007 to 2009 we found increased growth rates for all participating stations ranging

from $0.57\text{--}1.15\text{ }\text{yr}^{-1}$. The station with largest growth rate is Kiruna for which a positive value of $1.15 \pm 0.17\text{ }\text{yr}^{-1}$ is found. For comparison, Dlugokencky et al. (2009) report global averaged surface values of $0.47 \pm 0.03\text{ }\text{yr}^{-1}$ for 2007 and $0.25 \pm 0.03\text{ }\text{yr}^{-1}$ for 2008. The same authors also report a $0.78 \pm 0.07\text{ }\text{yr}^{-1}$ growth value for the polar northern latitudes in 2007 and $0.46 \pm 0.09\text{ }\text{yr}^{-1}$ for the low northern latitudes in 2008. The increased growth rates seen by Dlugokencky et al. (2009) for 2007 and 2008 is hence also observed at all FTIR stations.

5.3 N₂O trends

The fitted N₂O models are presented in Fig. 4 and the estimated trends are listed in Table 5. The N₂O trends vary from approximately $0.2 \pm 0.01\text{ }\text{yr}^{-1}$ at Jungfraujoch and Zugspitze to 0.29 ± 0.02 and $0.4 \pm 0.02\text{ }\text{yr}^{-1}$ at the two stations located further north. Earlier IPCC (2007) has reported a N₂O trend for the last decade of $0.26\text{ }\text{yr}^{-1}$. This trend is verified by in situ measurements by Haszpra et al. (2008) and total columns by Rinsland et al. (2009) who both report trends of $0.25 \pm 0.003\text{ }\text{yr}^{-1}$. The estimated N₂O trends for Jungfraujoch and Zugspitze are a bit weaker than the earlier reported trends but in close agreement to each other. The trends for Kiruna and especially Harestua are stronger than the reported trends and are not in agreement with each other. This trend discrepancy is unexpected since N₂O is well mixed in the atmosphere due to its tropospheric lifetime of 114 years (Davidson, 2009). To exclude that instrumental errors are the cause for the deviating N₂O trends we have estimated total column trends also for CO₂ from Harestua and Kiruna. CO₂ was used because its atmospheric circulation time is similar to the lifetime N₂O and that both of the species are measured with the same type of detector (InSb detector). The CO₂ retrieval was conducted in the $2620\text{--}2630\text{ cm}^{-1}$ region with Hitran08 line parameters (R. Kohlhepp and F. Hase, private communication, 2010). The estimated CO₂ trends for the two stations showed to be very similar, $0.50 \pm 0.06\text{ }\text{yr}^{-1}$ for Harestua and $0.56 \pm 0.04\text{ }\text{yr}^{-1}$ for Kiruna on a 2- σ basis and this corresponds well to the in situ trend of roughly 0.51 % presented by IPCC (2007) (the trend is based on an increase of 19 ppm from 1995 to 2005). From this test it is concluded that the FTIR instruments at Harestua and Kiruna behaved well during the studied period.

To further investigate the trend discrepancy between the FTIR stations trends we derived tropospheric- and stratospheric partial columns from the FTIR data at each station. The partial columns was derived with a weight function described by Gardiner et al. (2008) which use the average tropopause height and its standard deviation, here taken from the ECMWF model. The trends in the partial columns were estimated with a function consisting of a linear trend and a seasonal cycle with a phase. All the estimated tropospheric trends were in the range of $0.19 \pm 0.01\text{ }\text{yr}^{-1}$

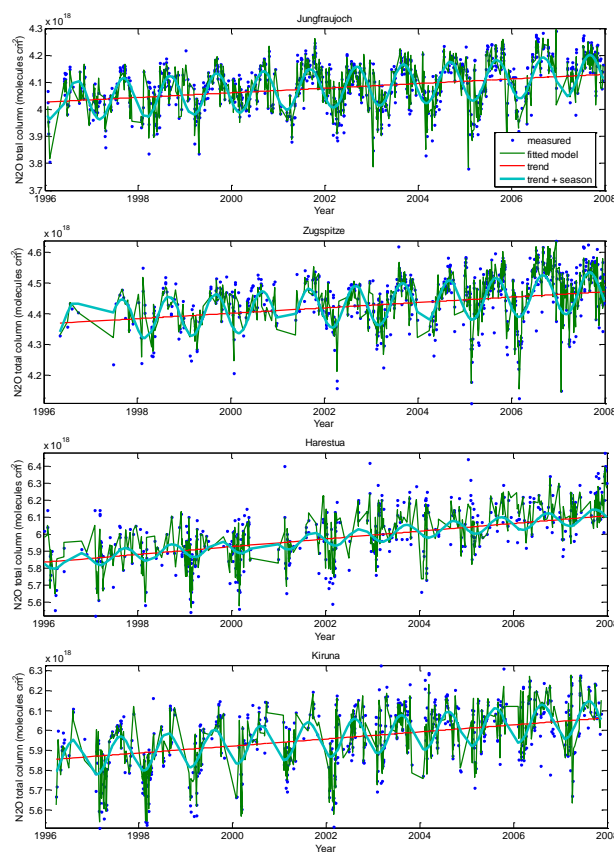


Fig. 4. As Fig. 3a but for N₂O total columns.

to $0.28 \pm 0.03\text{ }\text{yr}^{-1}$ while the stratospheric trends showed large inter station variability with strong positive trends at Harestua and Kiruna and weak positive trends at Jungfraujoch and Zugspitze, Table 6. Earlier, Gardiner et al. (2008) also showed this behaviour.

To verify the latitudinal differences in stratospheric N₂O trends detected by the solar FTIR measurements a comparison with N₂O limb measurements from the Odin satellite, see Sect. 3 was carried out. To get a rough estimation of the stratospheric N₂O columns at three locations (Jungfraujoch/Zugspitze, Harestua and Kiruna) SMR data were retrieved from altitudes covering 14–30 km within a radius of 500 km centred at each location. The satellite data quality in terms of measurement response and retrieval error were studied for all three locations and shown to be close to one and random scattered at approximately 10 % respectively. The stratospheric N₂O trends from the SMR instrument data were calculated with the same trend model as the tropospheric and stratospheric partial columns. The outcome of the trend study is presented in Table 6 and in Fig. 5. The rough FTIR-satellite comparison indicates that the stratospheric N₂O trends can vary with latitude. This has to the authors' knowledge not been reported before. The strongest positive trends for both FTIR and satellite data are estimated

Table 6. Stratospheric N₂O trends from SMR and FTIR data presented in % yr⁻¹. The trends are presented with associated 2- σ confidence intervals and use the 2005 average partial column as reference.

	Jungfraujoch	Zugspitze	Harestua	Kiruna
Odin/SMR (2001–2007)		0.27 ± 0.25	0.98 ± 0.28	0.60 ± 0.26
FTIR stratosphere (1996–2007)	0.15 ± 0.05	0.28 ± 0.07	1.13 ± 0.15	0.67 ± 0.12
FTIR troposphere (1996–2007)	0.27 ± 0.01	0.19 ± 0.01	0.28 ± 0.03	0.24 ± 0.03

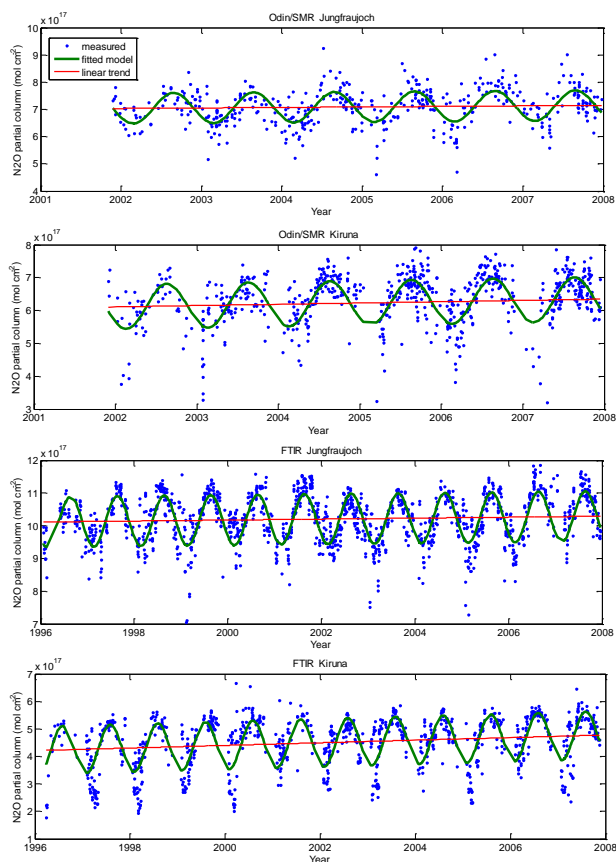


Fig. 5. Stratospheric partial columns of N₂O with fitted seasonal function and linear trend for Jungfraujoch and Kiruna from the SMR instrument onboard the Odin satellite and solar FTIR data.

at Harestua. A slightly weaker trend is seen in Kiruna and a much weaker trend is estimated in the Alp region. It hence seems that the difference in total column trends between the Alp region and Harestua and Kiruna is caused by the differences in the stratospheric column trends and it appears that the highest trend is found at the vortex edge, above Harestua as observed by FTIR and the SMR onboard Odin. We do not have an explanation for this behaviour but is likely related to the atmospheric circulation, since N₂O has a very long lifetime which would smooth out differences in sources and sinks.

5.4 Model stability

To obtain the confidence intervals, the residual from the model is assumed to be normally distributed with constant variance around a mean value of zero and to be free from autocorrelation. The residual distributions from the regression models for all FTIR stations are shown in the lower left panel in Fig. 6 (for CH₄) and in Fig. 7 (for N₂O), also presented is a normal distribution based on the standard deviation from each of the residuals. These distributions indicate that the assumption of normal distribution is justified. In the lower right panels in Figs. 6 and 7 the residuals are plotted as a function of the fitted model. To justify the constant variance assumption the residuals are expected to be randomly scattered around a constant level of zero. In our case we conclude that this assumption is justified for all the regression models. Also, to verify the assumption that no autocorrelation is present in the time series we look at the residual as a function of time, this can be seen in the upper panel in Figs. 6 and 7. Shapes such as cycles might indicate autocorrelation and may make the confidence intervals for the estimated trends larger. Based on the residual analysis we conclude that no strong autocorrelation is presented in any of the regression models.

When working with multiple regression models, one always needs to consider multicollinearity. Multicollinearity is when one or several of the independent variables in the regression model contain similar information, i.e. are linearly dependent. The presence of multicollinearity may result in physically unrealistic values or signs and large confidence intervals of the estimated regression coefficients. To investigate the presence of multicollinearity in the regression model the concept of the variance inflation factor, VIF factor, is used (Neter et al., 1990). A VIF factor of 1 indicates totally independent variables and a factor larger than 10 indicates serious multicollinearity in the model (Neter et al., 1990). In our case the calculated VIF factors are well below 10 for all FTIR stations and both of the species under investigation.

To verify that the 1 % criteria, earlier defined in Sect. 4.4, in the calculations of the anomalies is appropriate a sensitivity analysis is performed on all the regression models. In the analysis the estimated linear trend and the adjusted R^2 value is studied as the anomaly of one of the atmospheric parameters is changed, i.e. the order of the fitted polynomial to

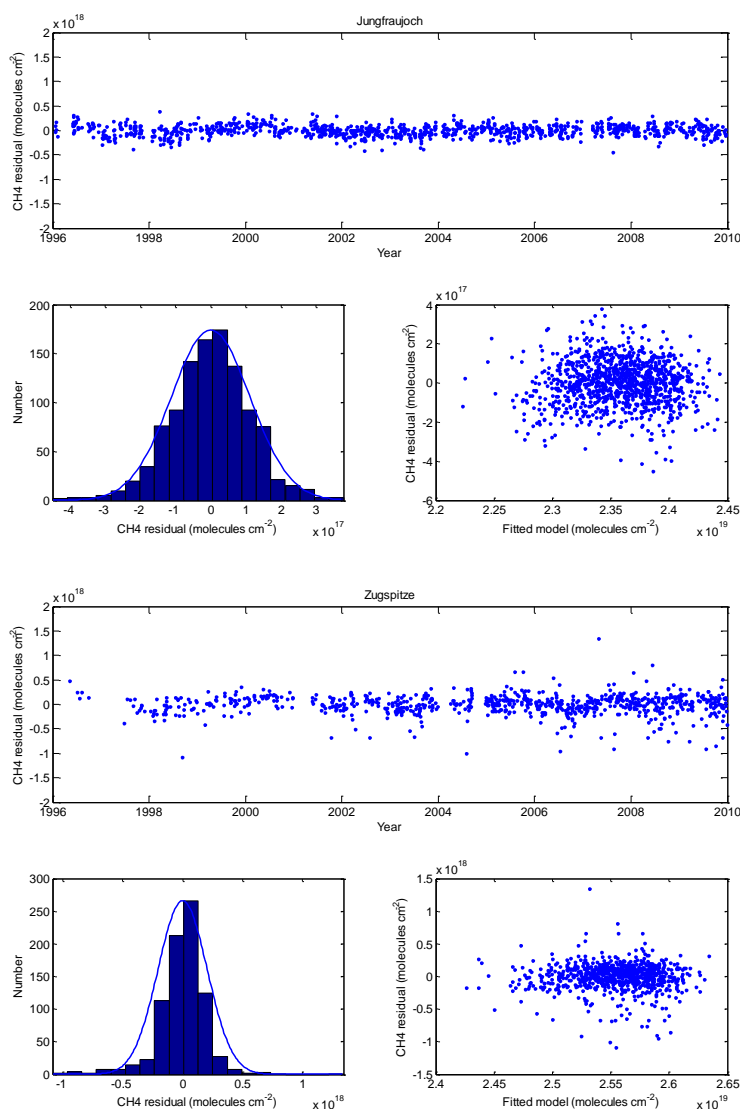


Fig. 6. CH₄ residuals and distributions of the Jungfraujoch and Zugspitze FTIR time series when a piecewise linear trend is used.

the parameter is changed. The change of the linear trend in the total columns of CH₄ and N₂O is largest when increasing from polynomial order zero to a first order and to a second order polynomial for the total column of HF (0, 1, 2) while for the other parameters the change is largest from zero to first (0,1). At higher order of polynomial only very small changes in the estimated trends are observed. It can also be seen that the adjusted R^2 value not increase for polynomials with higher order than two for HF and one for the other parameters. From the sensitivity analysis we conclude that the 1 % criterion is appropriate for deriving the anomalies.

5.5 Method comparison

The results of the multiple regression model has been compared to two other trend methods. The first method, re-

ferred to as the Bootstrap algorithm (Efron and Tibshirani, 1993; Gardiner et al., 2008), is based on the least squares fitting of a linear trend and a seasonal component to the data. From the residuals a large number of dataset is randomly sampled (Bootstrapped), these datasets represent the random effects in the data. Each of these dataset is then added to the original fitted function and a set of trends are estimated. The center point of the estimated trends represents the final trend estimation and the width is the confidence intervals. The bootstrap algorithm is a non parametric method since it does not rely on the normal distribution and equal variance assumption. The second tested trend method is a simple least squares fit of a straight line and a seasonal component including a phase, when using this method the normal distribution assumption is made. Linear trends were estimated by

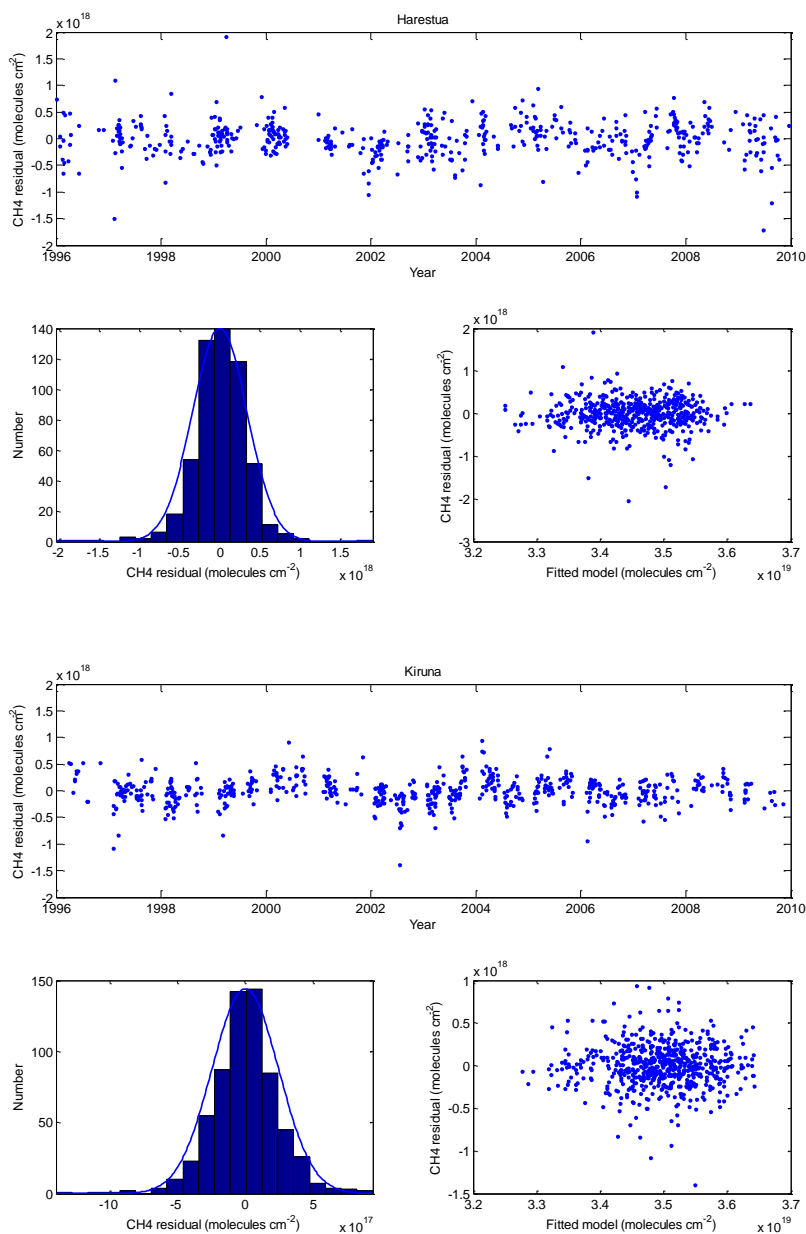


Fig. 6. Continued.

the multiple regression model, the Bootstrap algorithm and by the simple least squares fit of a straight line and a seasonal component, for the 1996–2009 and 1996–2007 period for CH₄ and N₂O total columns respectively. The outcome of the study is presented in Table 7 which shows the estimated trends with associated 95 % confidence limits. The three trend methods show all results that are in relatively close agreement to each other. In general, the multiple regression method has slightly smaller confidence intervals than the other two methods. The trends obtained from the Bootstrap algorithm and the model with a linear trend and sea-

sonal function are very similar for all the participating FTIR stations and both the CH₄ and N₂O time series. The reason for this is that all the CH₄ and N₂O time series are close to normal distributed. In this case the Bootstrap resampling stage is not necessary and can in fact introduce errors in the trend estimate since it can create physically unrealistic time series, especially for the stations at northern latitudes. One example is the high CH₄ and N₂O values related to the presence of the polar vortex, typically during winter and early spring, which with the Bootstrap algorithm can be located to the summer or autumn season. When fitting a trend to these

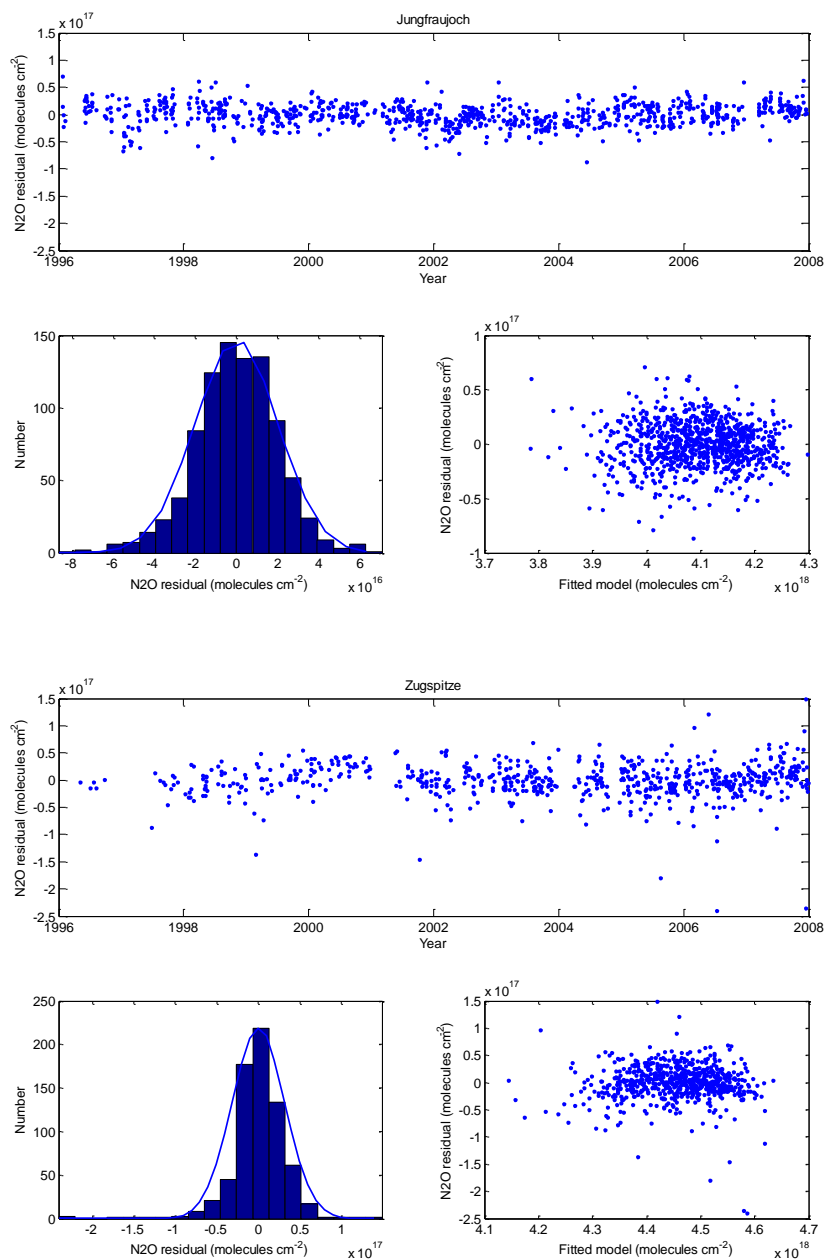


Fig. 7. N₂O residuals and distributions of the Jungfraujoch and Zugspitze FTIR time series.

time series the estimated trend values will have an impact on the final trend result and potentially make the confidence intervals wider.

The trends estimated from the multiple regression method differ in magnitude with up to 31 % and have an uncertainty that differs up to 300 % compared to the other two methods. This difference is most likely because the multiple regression model takes the atmospheric variability into account and hence reduces the unexplained part of the trend model. From the method comparison and model stability analysis we con-

clude that the multiple regression model gives the most reliable trends since it takes the atmospheric variability into account and fulfils the statistical assumptions presented in Sect. 5.4.

6 Discussion and conclusion

Long term CH₄ and N₂O trends from solar FTIR total columns have been estimated at four European stations. The estimated trends show latitudinal differences with stronger

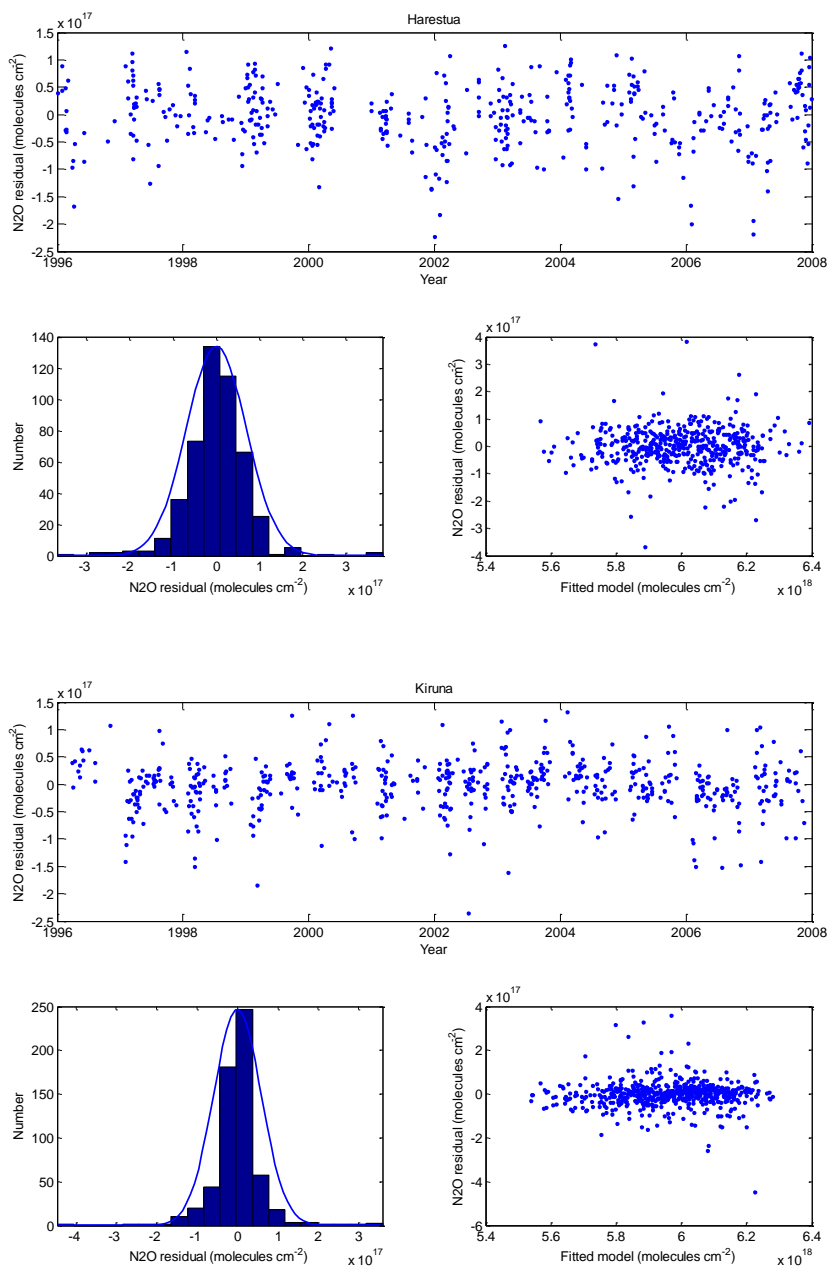


Fig. 7. Continued.

trends for both species at the northern sites and weaker trends at the Alpine stations.

When it comes to CH₄ this latitudinal difference is not surprising since the atmospheric concentration of the species are highly influenced by local sources. At high latitudes wetland contributes up to 25 % of the CH₄ total emissions and these wetlands have shown to be sensitive to climate change (Jackowicz-Korczynski et al., 2010). In addition Russian natural gas is produced at the same latitudes as Harestua and Kiruna. These might be two possible rea-

sons for the stronger trends detected at the northern latitude sites (Harestua and Kiruna) compared to the two Alpine stations.

The latitudinal difference in the estimated N₂O trends is compared to CH₄ unexpected. Atmospheric N₂O has a lifetime that is more than 12 times longer than that of CH₄, 120 years instead of 9, and is thereby well mixed in the troposphere and relatively insensitive to local sources. In the Odin SMR comparison we conclude that the strong FTIR total column trends at Harestua and Kiruna most probably arise from very strong stratospheric trends at these sta-

Table 7. Estimated linear trends from the total columns of CH₄ and N₂O. The trends are presented in percent per year (% yr⁻¹) with the reference year given as the average value of year 2000. All trends are given with associated 95 σ confidence limits.

Trend model	Species	Jungfrauoch	Zugspitze	Harestua	Kiruna
Multiple regression model	CH ₄	0.16 ± 0.01	0.13 ± 0.01	0.25 ± 0.02	0.21 ± 0.01
	N ₂ O	0.21 ± 0.01	0.19 ± 0.01	0.40 ± 0.02	0.29 ± 0.02
Bootstrap algorithm	CH ₄	0.16 ± 0.02	0.09 ± 0.03	0.28 ± 0.04	0.26 ± 0.04
	N ₂ O	0.25 ± 0.03	0.22 ± 0.03	0.45 ± 0.06	0.33 ± 0.05
Linear trend with seasonal component	CH ₄	0.16 ± 0.01	0.09 ± 0.02	0.28 ± 0.03	0.26 ± 0.02
	N ₂ O	0.25 ± 0.02	0.22 ± 0.02	0.46 ± 0.04	0.34 ± 0.03

tions. One possible explanation could be the strengthening of the Brewer Dobson circulation as described by Li et al. (2010). This circulation transports air masses from the tropical tropopause into the stratosphere and towards the poles. If the circulation gets stronger with time more N₂O is transported towards Harestua and Kiruna with a stratospheric trend as result. The stations located further south are less influenced by this transport and hence a weaker stratospheric trend is detected. Another possible reason to the trend differences could be a trend in the tropopause height due to climate change or other changes in the atmospheric dynamics. Linear trends were therefore estimated from the tropopause data, the earlier used ECMWF data, for the FTIR stations. All the estimated trends were close to zero and insignificant. From this we conclude that a change in the tropopause altitude is most likely not responsible for the stratospheric N₂O trends. We conclude that more studies are needed regarding the latitudinal difference in stratospheric N₂O.

Acknowledgements. This paper is funded by the EU project HYMN. The author would like to thank Anders Strandberg and Glenn Persson for Harestua FTIR measurement and Marston Johnston for ECMWF data. P. Duchatelet and E. Mahieu have further been supported by the Belgian Federal Science Policy Office (BEL-SPO, Brussels). The International Foundation High Altitude Research Stations Jungfrauoch and Gornergrat (HFSJG, Bern) is also acknowledged. T. Blumenstock, F. Hase and M. Schneider would like to thank the Institute of Space Physics (IRF) Kiruna and in particular Uwe Raffalski (IRF) for supporting the measurements at Kiruna. Odin is a Swedish-led satellite project funded jointly by the Swedish National Space Board (SNSB), the Canadian Space Agency (CSA), the Centre National d'Etudes Spatiales (CNES) in France and the National Technology Agency of Finland (Tekes). The Odin mission is since 2007 supported through the 3rd party mission programme of the European Space Agency (ESA).

Edited by: C. Gerbig

References

- Bates, D. R. and Hays, P. B.: Atmospheric Nitrous Oxide, *Planet. Space Sci.*, 15, 189–197, 1967.
- Davidson, E. A.: The contribution of manure and fertilizer nitrogen to atmospheric nitrous oxide since 1860, *Nat. Geosci.*, 2, 659–662, doi:10.1038/Ngeo608, 2009.
- DeMazière, M., Vigouroux, C., Gardiner, T., Coleman, M., Woods, P., Ellingsen, K., Gauss, M., Isaksen, I., Blumenstock, T., Hase, F., Kramer, I., Camy-peyret, C., Chelin, P., Mahieu, E., Demoulin, P., Duchatelet, P., Mellqvist, J., Strandberg, A., Velazco, V., Notholt, J., Sussmann, R., Stremme, W., and Rockmann, A.: The exploitation of ground-based Fourier transform infrared observations for the evaluation of tropospheric trends of greenhouse gases over Europe, *Environm. Sci.*, 2, 283–293, 2005.
- Dlugokencky, E. J., Steele, L. P., Lang, P. M., and Masarie, K. A.: The Growth-Rate and Distribution of Atmospheric Methane, *J. Geophys. Res.-Atmos.*, 99, 17021–17043, 1994.
- Dlugokencky, E. J., Houweling, S., Bruhwiler, L., Masarie, K. A., Lang, P. M., Miller, J. B., and Tans, P. P.: Atmospheric methane levels off: Temporary pause or a new steady-state?, *Geophys. Res. Lett.*, 30, 1992, doi:10.1029/2003gl018126, 2003.
- Dlugokencky, E. J., Bruhwiler, L., White, J. W. C., Emmons, L. K., Novelli, P. C., Montzka, S. A., Masarie, K. A., Lang, P. M., Crotwell, A. M., Miller, J. B., and Gatti, L. V.: Observational constraints on recent increases in the atmospheric CH₄ burden, *Geophys. Res. Lett.*, 36, L18803, doi:10.1029/2009gl039780, 2009.
- Efron, B. and Tibshirani, R.: An introduction to the bootstrap, *Monographs on statistics and applied probability*, 57, Chapman & Hall, New York, USA, xvi, 436 pp., 1993.
- Gardiner, T., Forbes, A., de Mazière, M., Vigouroux, C., Mahieu, E., Demoulin, P., Velazco, V., Notholt, J., Blumenstock, T., Hase, F., Kramer, I., Sussmann, R., Stremme, W., Mellqvist, J., Strandberg, A., Ellingsen, K., and Gauss, M.: Trend analysis of greenhouse gases over Europe measured by a network of ground-based remote FTIR instruments, *Atmos. Chem. Phys.*, 8, 6719–6727, doi:10.5194/acp-8-6719-2008, 2008.
- Hase, F., Blumenstock, T., and Paton-Walsh, C.: Analysis of the instrumental line shape of high-resolution Fourier transform IR spectrometers with gas cell measurements and new retrieval software, *Appl. Optics*, 38, 3417–3422, 1999.
- Hase, F., Hannigan, J. W., Coffey, M. T., Goldman, A., Hopfner,

- M., Jones, N. B., Rinsland, C. P., and Wood, S. W.: Intercomparison of retrieval codes used for the analysis of high-resolution, ground-based FTIR measurements, *J. Quant. Spectrosc. Ra.*, 87, 25–52, doi:10.1016/j.jqsrt.2003.12.008, 2004.
- Haszpra, L., Barcza, Z., Hidy, D., Szilagyi, I., Dlugokencky, E., and Tans, R.: Trends and temporal variations of major greenhouse gases at a rural site in Central Europe, *Atmos. Environ.*, 42, 8707–8716, doi:10.1016/j.atmosenv.2008.09.012, 2008.
- IPCC: Contribution of Working Group I to the Fourth Assessment Report of the Intergovernmental Panel on Climate Change, 2007, Cambridge University Press, Cambridge, United Kingdom and New York, NY, USA, 2007.
- Jackowicz-Korczynski, M., Christensen, T. R., Backstrand, K., Crill, P., Friborg, T., Mastepanov, M., and Strom, L.: Annual cycle of methane emission from a subarctic peatland, *J. Geophys. Res.-Biogeo.*, 115, G02009, doi:10.1029/2008jg000913, 2010.
- Jones, A., Urban, J., Murtagh, D. P., Eriksson, P., Brohede, S., Haley, C., Degenstein, D., Bourassa, A., von Savigny, C., Sonkaew, T., Rozanov, A., Bovensmann, H., and Burrows, J.: Evolution of stratospheric ozone and water vapour time series studied with satellite measurements, *Atmos. Chem. Phys.*, 9, 6055–6075, doi:10.5194/acp-9-6055-2009, 2009.
- Li, F., Newman, P. A., and Stolarski, R. S.: Relationships between the Brewer-Dobson circulation and the southern annular mode during austral summer in coupled chemistry-climate model simulations, *J. Geophys. Res.-Atmos.*, 115, D15106, doi:10.1029/2009jd012876, 2010.
- Mellqvist, J., Galle, B., Blumenstock, T., Hase, F., Yashcov, D., Notholt, J., Sen, B., Blavier, J.-F., Toon, G. C., and Chipperfield, M. P.: Ground-Based FTIR observations of chlorine activation and ozone depletion inside the Arctic vortex during the winter of 1999/2000, *J. Geophys. Res.*, 107, 8263, doi:10.1029/2001JD001080, 2002.
- Montgomery, D. C., Jennings, C. L., and Kulahci, M.: Introduction to time series analysis and forecasting, in: *Wiley series in probability and statistics*, edited by: Hoboken, N. J., Wiley-Interscience, xi, 445 pp., 2008.
- Murtagh, D., Frisk, U., Merino, F., Ridal, M., Jonsson, A., Stegman, J., Witt, G., Eriksson, P., Jimenez, C., Megie, G., de la Noe, J., Ricaud, P., Baron, P., Pardo, J. R., Hauchorne, A., Llewellyn, E. J., Degenstein, D. A., Gattinger, R. L., Lloyd, N. D., Evans, W. F. J., McDade, I. C., Haley, C. S., Sioris, C., von Savigny, C., Solheim, B. H., McConnell, J. C., Strong, K., Richardson, E. H., Leppelmeier, G. W., Kyrola, E., Auvinen, H., and Oikarinen, L.: An overview of the Odin atmospheric mission, *Can. J. Phys.*, 80, 309–319, doi:10.1139/P01-157, 2002.
- Neter, J., Wasserman, W., and Kutner, M. H.: *Applied linear statistical models : regression, analysis of variance, and experimental designs*, 3rd edn., Irwin, Homewood, IL, xvi, 1181 pp., 1990.
- Rinsland, C. P., Jones, N. B., Connor, B. J., Logan, J. A., Pougatchev, N. S., Goldman, A., Murcray, F. J., Stephen, T. M., Pine, A. S., Zander, R., Mahieu, E., and Demoulin, P.: Northern and southern hemisphere ground-based infrared spectroscopic measurements of tropospheric carbon monoxide and ethane, *J. Geophys. Res.-Atmos.*, 103, 28197–28217, 1998.
- Rinsland, C. P., Chiou, L., Boone, C., Bernath, P., Mahieu, E., and Zander, R.: Trend of lower stratospheric methane (CH₄) from atmospheric chemistry experiment (ACE) and atmospheric trace molecule spectroscopy (ATMOS) measurements, *J. Quant. Spectrosc. Ra.*, 110, 1066–1071, doi:10.1016/j.jqsrt.2009.03.024, 2009.
- Rodgers, C. D.: *Inverse Methods for Atmospheric Sounding, Series on Atmospheric, Oceanic and Planetary Physics*, 2, 55–63, 2000.
- Simpson, I. J., Rowland, F. S., Meinardi, S., and Blake, D. R.: Influence of biomass burning during recent fluctuations in the slow growth of global tropospheric methane, *Geophys. Res. Lett.*, 33, L22808, doi:10.1029/2006gl027330, 2006.
- Strong, K., Wolff, M. A., Kerzenmacher, T. E., Walker, K. A., Bernath, P. F., Blumenstock, T., Boone, C., Catoire, V., Coffey, M., De Mazire, M., Demoulin, P., Duchatelet, P., Dupuy, E., Hannigan, J., Hpfner, M., Glatthor, N., Griffith, D. W. T., Jin, J. J., Jones, N., Jucks, K., Kuellmann, H., Kuttippurath, J., Lambert, A., Mahieu, E., McConnell, J. C., Mellqvist, J., Mikuteit, S., Murtagh, D. P., Notholt, J., Piccolo, C., Raspollini, P., Ridolfi, M., Robert, C., Schneider, M., Schrems, O., Semeniuk, K., Senten, C., Stiller, G. P., Strandberg, A., Taylor, J., Tétard, C., Toohey, M., Urban, J., Warneke, T., and Wood, S.: Validation of ACE-FTS N₂O measurements, *Atmos. Chem. Phys.*, 8, 4759–4786, doi:10.5194/acp-8-4759-2008, 2008.
- Sussmann, R. and Borsdorff, T.: Technical Note: Interference errors in infrared remote sounding of the atmosphere, *Atmos. Chem. Phys.*, 7, 3537–3557, doi:10.5194/acp-7-3537-2007, 2007.
- Sussmann, R., Stremme, W., Buchwitz, M., and de Beek, R.: Validation of ENVISAT/SCIAMACHY columnar methane by solar FTIR spectrometry at the Ground-Truthing Station Zugspitze, *Atmos. Chem. Phys.*, 5, 2419–2429, doi:10.5194/acp-5-2419-2005, 2005.
- Tiao, G. C., Reinsel, G. C., Xu, D. M., Pedrick, J. H., Zhu, X. D., Miller, A. J., Deluisi, J. J., Mateer, C. L., and Wuebbles, D. J.: Effects of Autocorrelation and Temporal Sampling Schemes on Estimates of Trend and Spatial Correlation, *J. Geophys. Res.-Atmos.*, 95, 20507–20517, 1990.
- Toon, G. C., Blavier, J.-F., Sen, B., Salawitch, R. J., G. B. Osterman, Notholt, J., Rex, M., McElroy, C. T., and Russell, J. M.: Ground-based observations of Arctic O₃ loss during spring and summer 1997, *J. Geophys. Res.*, 104, 497–510, 1997.
- Twomey, S.: *Introduction to the mathematics of inversion in remote sensing and indirect measurements*, Dover Publications, Mineola, N.Y., x, 237 pp., 1996.
- Urban, J., Lautie, N., Le Flochmoen, E., Jimenez, C., Eriksson, P., de La Noe, J., Dupuy, E., Ekstrom, M., El Amraoui, L., Frisk, U., Murtagh, D., Olberg, M., and Ricaud, P.: Odin/SMR limb observations of stratospheric trace gases: Level 2 processing of ClO, N₂O, HNO₃, and O-3, *J. Geophys. Res.-Atmos.*, 110, D14307, doi:10.1029/2004jd005741, 2005a.
- Urban, J., Lautie, N., Le Flochmoen, E., Jimenez, C., Eriksson, P., de La Noe, J., Dupuy, E., El Amraoui, L., Frisk, U., Jegou, F., Murtagh, D., Olberg, M., Ricaud, P., Camy-Peyret, C., Dufour, G., Payan, S., Huret, N., Pirre, M., Robinson, A. D., Harris, N. R. P., Bremer, H., Kleinbohl, A., Kullmann, K., Kunzi, K., Kuttippurath, J., Ejiri, M. K., Nakajima, H., Sasano, Y., Sugita, W., Yokota, T., Piccolo, C., Raspollini, P., and Ridolfi, M.: Odin/SMR limb observations of stratospheric trace gases: Validation of N₂O, *J. Geophys. Res.-Atmos.*, 110, D09301, doi:10.1029/2004jd005394, 2005b.
- Urban, J., Murtagh, D., Lautié, N., Barret, B., Dupuy, E., de La Noë, J., Eriksson, P., Frisk, U., Jones, A., Le Flochmoën, E., Olberg, M., Piccolo, C., Ricaud, P., and Rösevall, J.: Odin/SMR Limb

- Observations of Trace Gases in the Polar Lower Stratosphere during 2004–2005, Proc. ESA First Atmospheric Science Conference, edited by: Lacoste, H., ESA-SP-628, ISBN-92-9092-939-1, 2006.
- Weatherhead, E. C., Reinsel, G. C., Tiao, G. C., Meng, X. L., Choi, D. S., Cheang, W. K., Keller, T., DeLuisi, J., Wuebbles, D. J., Kerr, J. B., Miller, A. J., Oltmans, S. J., and Frederick, J. E.: Factors affecting the detection of trends: Statistical considerations and applications to environmental data, *J. Geophys. Res.-Atmos.*, 103, 17149–17161, 1998.
- Vigouroux, C., De Mazière, M., Demoulin, P., Servais, C., Hase, F., Blumenstock, T., Kramer, I., Schneider, M., Mellqvist, J., Strandberg, A., Velazco, V., Notholt, J., Sussmann, R., Stremme, W., Rockmann, A., Gardiner, T., Coleman, M., and Woods, P.: Evaluation of tropospheric and stratospheric ozone trends over Western Europe from ground-based FTIR network observations, *Atmos. Chem. Phys.*, 8, 6865–6886, doi:10.5194/acp-8-6865-2008, 2008.
- Yurganov, L. N., Blumenstock, T., Grechko, E. I., Hase, F., Hyer, E. J., Kasischke, E. S., Koike, M., Kondo, Y., Kramer, I., Leung, F. Y., Mahieu, E., Mellqvist, J., Notholt, J., Novelli, P. C., Rinsland, C. P., Scheel, H. E., Schulz, A., Strandberg, A., Sussmann, R., Tanimoto, H., Velazco, V., Zander, R., and Zhao, Y.: A quantitative assessment of the 1998 carbon monoxide emission anomaly in the Northern Hemisphere based on total column and surface concentration measurements, *J. Geophys. Res.-Atmos.*, 109, D15305, doi:10.1029/2004jd004559, 2004.
- Yurganov, L. N., Duchatelet, P., Dzhola, A. V., Edwards, D. P., Hase, F., Kramer, I., Mahieu, E., Mellqvist, J., Notholt, J., Novelli, P. C., Rockmann, A., Scheel, H. E., Schneider, M., Schulz, A., Strandberg, A., Sussmann, R., Tanimoto, H., Velazco, V., Drummond, J. R., and Gille, J. C.: Increased Northern Hemispheric carbon monoxide burden in the troposphere in 2002 and 2003 detected from the ground and from space, *Atmos. Chem. Phys.*, 5, 563–573, doi:10.5194/acp-5-563-2005, 2005.